Title	Possible involvement of iron-induced oxidative insults in neurodegeneration.
Author(s)	Asano, Takeshi; Koike, Masato; Sakata, Shin-ichi; Takeda, Yukiko; Nakagawa, Tomoko; Hatano, Taku; Ohashi, Satoshi; Funayama, Manabu; Yoshimi, Kenji; Asanuma, Masato; Toyokuni, Shinya; Mochizuki, Hideki; Uchiyama, Yasuo; Hattori, Nobutaka; Iwai, Kazuhiro
Citation	Neuroscience letters (2015), 588: 29-35
Issue Date	2015-02-19
URL	http://hdl.handle.net/2433/201603
Right	
Type	Journal Article
Textversion	author

Possible involvement of iron-induced oxidative insults in neurodegeneration

Takeshi Asano[a, b, 1], Masato Koike[c, 1], Shin-ichi Sakata[a], Yukiko Takeda[a, b, d], Tomoko Nakagawa[a, d], Taku Hatano[e], Satoshi Ohashi[e], Manabu Funayama[f], Kenji Yoshimi[g], Masato Asanuma[h], Shinya Toyokuni[i], Hideki Mochizuki[e, j], Yasuo Uchiyama[c], Nobutaka Hattori[e, *], and Kazuhiro Iwai[a, b, d, *]

[a]Department of Biophysics and Biochemistry, Graduate School of Medicine and Cell Biology and Metabolism Group, Graduate School of Frontier Biosciences, Osaka University, Suita, Osaka 565-0871, Japan
[b]CREST, Japan Science and Technology Agency, Kawaguchi, Saitama 332-0012, Japan
[c]Department of Cell Biology and Neuroscience, Juntendo University School of Medicine, Bunkyo-ku, Tokyo 113-8421, Japan
[d]Department of Molecular and Cellular Physiology, Graduate School of Medicine, Kyoto University, Sakyo-ku, Kyoto 606-8501, Japan
[e]Department of Neurology, [f]Research Institute for Diseases of Old Age, and [g]Department of Neurophysiology, Juntendo University, School of Medicine, Bunkyo-ku, Tokyo 113-8421, Japan
[h]Department of Brain Science, Graduate School of Medicine, Dentistry and Pharmaceutical Sciences, Okayama University, Okayama 700-8558, Japan
[i]Department of Pathology and Biological Responses, Graduate School of Medicine, Nagoya University Nagoya, Aichi 466-8550, Japan
[j]Department of Neurology, Graduate School of Medicine, Osaka University, Suita, Osaka 565-0871, Japan.

[1]These authors equally contributed to this study.

* Corresponding authors at: Department of Molecular and Cellular Physiology, Graduate School of Medicine, Kyoto University, Sakyo-ku, Kyoto 606-8501, Japan. Tel: +81 75 753 4671; fax: +81 75 753 4676.
E-mail address: kiwai@mcp.med.kyoto-u.ac.jp (K. Iwai)

or
Department of Neurology, Juntendo University, School of Medicine, Bunkyo-ku, Tokyo 113-8421, Japan. Tel: +81 3 3813 3111 ext. 3321; Fax: +81 3 5800 0547.
E-mail address: nhattori@juntendo.ac.jp (N. Hattori)

Keywords; iron; iron regulatory protein; oxidative stress; mitochondria; Parkin; Parkinson's disease

Abstract

Involvement of iron in the development of neurodegenerative disorders has long been suggested, and iron that cannot be stored properly is suggested to induce iron toxicity. To enhance iron uptake and suppress iron storage in neurons, we generated transgenic (Tg) mice expressing iron regulatory protein 2 (IRP2), a major regulator of iron metabolism, in a neuron-specific manner. Although very subtle, IRP2 was expressed in all regions of brain examined. In the Tg mice, mitochondrial oxidative insults were observed including generation of 4-hydroxynonenal modified proteins, which appeared to be removed by a mitochondrial quality control protein Parkin. Inter-crossing of the Tg mice to Parkin knockout mice perturbed the integrity of neurons in the substantia nigra and provoked motor symptoms. These results suggest that a subtle, but chronic increase in IRP2 induces mitochondrial oxidative insults and accelerates neurodegeneration in a mouse model of Parkinson's disease. Thus, the IRP2 Tg may be a useful tool to probe the roles of iron-induced mitochondrial damages in neurodegeraration research.

1. Introduction

Iron is an essential nutrient but can also be toxic because iron can readily cycle between ferrous (Fe^{2+}) and ferric (Fe^{3+}) in physiological settings and oxidizes proteins and nucleic acids via generation of free radicals. Dysregulation of iron metabolism causes some neurodegenerative diseases [21] and iron progressively accumulates in the lesions of sporadic neurodegenerative diseases such as Alzheimer's disease and Parkinson's disease [17, 18]. Therefore, tight regulation of iron metabolism appears to be critical for maintenance of neuronal cells [2, 21].

Iron homeostasis is mainly regulated by coordinated expression of molecules involved in iron uptake and storage. Iron availability is regulated at the post-transcriptional level through the interactions between the iron-responsive elements (IREs) on mRNAs encoding proteins involved in iron metabolism and mRNA-binding proteins called iron regulatory proteins (IRPs) [14]. Binding of IRPs to IREs on the mRNA of the iron uptake protein, transferrin receptor1 (TfR1) enhances translation of TfR1, whereas binding of IRPs to the IRE on the mRNA of the iron storage protein, ferritin suppresses its production. Iron stored in ferritin is not toxic, because Fe^{3+} stored in ferritin cannot be converted to Fe^{2+}. Therefore, augmented expression of IRPs leads to an increase in iron uptake and a decrease in iron storage, which result in an increase of iron that cannot be stored safely and able to oxidize and damage cellar components [10]. There are two IRPs (IRP1 and IRP2) and IRP2 is abundant in brain as compared to other organs [9].

To examine the effect of iron in the integrity of neurons in mice, we generated transgenic (Tg) mice that express IRP2 in neurons [4]. We show increase in IRP2 induces mitochondrial oxidative insults and accelerates neurodegeneration.

2. Material and methods

2.1 Antibodies

The anti-myc (4A6 and 9E10) were purchased from Millipore and Roche, respectively. The following antibodies were obtained as indicated: 4-hydroxynonenal (4-HNE) (JaICA and Alpha diagnostic); β-actin, Tom20 (Santa Cruz Biotechnology); PINK1 (Novus); HA (Covance); COX III core1 (Invitrogen); and tubulin, Tyrosine hydroxylase (TH) (Cedarlane). Anti-IRP2 has been described [1].

2.2 Plasmids and cell culture

HA- and GFP-human Parkin was subcloned into pDNA3.1 (invitrogen) and pTRE2 (Clontech), respectively. p220-IRP2-myc has been described previously [6]. pNSE-IRP2-myc was generated by subcloning the human IRP2-myc cDNA into pNSE [4]. pcDNA3.1-HA- or pTRE2-GFP-Parkin were stably introduced in HEK293 or HeLa cells, respectively using Lipofectamine 2000 (Invitrogen). Parkin expression was induced by addition of 1 μg/ml doxycycline (DOX) for 48 h in HeLa cells that expressed GFP-Parkin in a DOX-dependent manner. IRP2-myc under the control of dexamethasone (DEX) (p220-IRP2-myc) was induced by treatment with 80 nM DEX for 48 h.

2.3 Immunoblotting, immunoprecipitation and fluorescence microscopy

These analyses were performed as described previously [19]. Quantifications were performed by Fluoview (Olympus) and BZ-II Analyzer (Keyence).

2.4 Assessment of mitochondrial membrane potential

Cells were treated with 25 nM MitoTracker Orange for 10 min at 37°C.

2.5 Generation of NSE-IRP2 Tg mice

NSE-IRP2 transgenic mice were generated by microinjection of pNSE-IRP2-myc into E0.5 mouse embryos from a C57BL/6J × DBA2/J F1 background. Parkin KO mice have been described [15]. These mice were backcrossed to C57BL/6J mice (Charles River Japan) more than ten times. All the experiments using mice were carried out according to the Guidelines for Animal Experimentation, Juntendo, Osaka, and Kyoto University.

2.6 Southern blotting

Southern blotting was performed as previously described using human IRP2 cDNA as a probe [19].

2.7 RNA electrophoretic mobility shift assay (EMSA)

EMSA was performed as described previously [6].

2.8 Histochemical and morphological analyses

Brain sections were stained with the appropriate primary antibodies, followed by development using HISTOFINE (Nichirei) and a metal-enhanced diaminobenzidine (DAB) substrate kit (Pierce). Toluidine blue staining and electron microscopy were performed as described previously [7].

2.9 Fe^{2+} staining

Brains were perfused consecutively with 50 mM hydrogen sulfide and 4% paraformaldehyde, embedded in paraffin. Sections were immersed in a solution of 5% $K_3[Fe(CN)_6]$ and 5% HCl followed by immersion in 0.05% DAB and in 1% H_2O_2 plus 0.05% DAB.

2.10 Measurement of striatal dopamine, 3, 4-dihydroxyphenylacetic acid (DOPAC), and homovanillic acid (HVA)

Dissected striata were analyzed using a reverse-phase C18 column (150 × 4.6 mm; Tosoh) on an HPLC system (ESA Biosciences) with a coulometric 8-electrode electrochemical detection system.

2.11 Behavioral analyses

A 40 cm × 40 cm square open field with 10 cm × 10 cm grids was used for the open-field test.

2.12 Administration of desferrioxamine (DFO)

Saline containing 300 mg/kg DFO was injected intraperitoneally into mice once a day for 10 consecutive days.

2.13 Statistical analysis

Statistical significance was determined using a one-way ANOVA. Data are shown by mean ± SEM.

3. Results

3.1 A subtle increase in IRP2 induces oxidative insults in neurons

To probe the effect of iron in the integrity of neurons, we generated Tg mice expressing IRP2-myc using the rat NSE promoter because induced expression of IRP2 increases TfR1 expression and decreases ferritin expression, thereby increases the amount of iron that are not stored safely (Fig. 1A). Two lines of Tg mice exhibited identical phenotypes and Line 26 was analyzed here (Fig. 1B and C). IRP2 is stabilized in iron-depleted condition [14]. IRP2-myc was expressed in all areas in the brain examined, including the SN of NSE-IRP2 Tg mice treated with an iron-chelator, DFO (Fig. 1D). IRP2-myc expressed in the brain exhibited IRE-binding activity (Fig. 1E). The amount of exogenous IRP2 (Fig. 1C, top panel) was very small compared to endogenous IRP2 and an increase in total IRP2 levels could not be detectable in NSE-IRP2 Tg mice brain using conventional immunoblotting (Fig. 1C, bottom panel), which might be attributed to the observation that mice expressing a large amount of IRP2 might not be viable [10]. To probe the amount of iron that is potentially harmful to cells, levels of Fe^{2+}, which can cycle between Fe^{2+} and Fe^{3+}, were probed. Increase of Fe^{2+} was observed in all regions of the brain of 12-month-old NSE-IRP2 Tg mice, including the SN (Fig. 1F). The activity of TH, a critical enzyme for catecholamine synthesis, is enhanced by iron [12]. The amount of TH in the striatum increased in NSE-IRP2 Tg mice (Fig. 1G), confirming an increase in available iron in NSE-IRP2 Tg neurons. Modification of proteins by 4-HNE, a major product of lipid peroxidation, is one of the most reliable markers of oxidative insults to proteins [20]. Anti-4-HNE immunoreactivity which represents 4-HNE-modified proteins [20], was increased in all areas of the brain examined in 18-month-old NSE-IRP2 Tg mice (Fig. 1H). These data suggest that although subtle, chronic expression of exogenous IRP2 can provoke oxidative insults in neurons possibly by increasing the amount of iron that are not stored safely.

3.2 Induced expression of IRP2 augments mitochondrial oxidative damage

Since 4-HNE modification seems to provoke dysfunction of mitochondrial proteins [13], subcellular localization of 4-HNE-modified proteins induced by iron was probed using HEK293 cells that expressed IRP2 in an inducible manner. 4-HNE immunoreactivity detected in IRP2-expressing cells treated with iron source, ferric ammonium citrate (FAC) was co-localized with the mitochondria marker Tom20 (Fig. 2A-C). Mitochondrial membrane potential is an important indicator of mitochondrial integrity [11]. A substantial fraction of mitochondria did not stain with MitoTracker, which is known to accumulate to mitochondria with intact membrane

potential, in IRP2-expressing cells treated with iron (Fig. 2D). These results indicate that enhanced IRP2 expression decreases its membrane potential.

Decrease in mitochondrial membrane potential triggers stabilization of PINK1 kinase in mitochondria and subsequent recruitment of the Parkin ubiquitin ligase to mitochondria, which is suggested to be crucial for the maintenance of mitochondrial integrity [8, 11]. PINK1 was stabilized in and Parkin was recruited to mitochondria in FAC-treated cells expressing exogenous IRP2 (Fig. 2E). We then examined the involvement of Parkin in the removal of mitochondrial 4-HNE-modifed proteins using HeLa cells that lack Parkin expression [8]. Although 4-HNE-immunoreactivity was not detected in HeLa cells treated with FAC alone, exogenous IRP2 induced 4-HNE signals that co-localized with Tom20 in FAC-treated HeLa cells. The mitochondrial 4-HNE signal induced by exogenous IRP2 and iron was eliminated by introduction of Parkin (Fig. 2F and G). These results suggest that Parkin is involved in the clearance of oxidatively modified proteins generated by IRP2 and iron in mitochondria.

3.3 Increased mitochondrial oxidative insults and neurodegeneration in the SN of NSE-IRP2 Tg × Parkin KO mice

Although 4-HNE modification could not be detected without adding exogenous iron in cultured cells (Fig. 2A), 4-HNE modification could be observed in mouse neurons with enhanced expression of IRP2 alone (Fig. 1H). Iron is essential nutrient for cell proliferation, whereas, neurons are regarded as quiescent cells [5]. Then the effect of IRP2 expression on mitochondrial oxidative damages in neurons was probed in 6-month-old mice. As shown in Fig. 3A and B, no overt 4-HNE immunoreactivity could be detected in the SN of NSE-IRP2 Tg mice. However, the 4-HNE immunoreactivity, which was co-localized with a mitochondrial protein, COX III, was prominently detected in the SN neurons of NSE-IRP2 Tg × Parkin KO mice [15]. These results suggested that IRP2 expression provokes mitochondrial oxidative insults and Parkin is involved in the removal of the mitochondrial insults in the SN. Consistent with these results, degenerated neurons, which stain intensely with toluidine blue, were observed in the SN of 6-month-old NSE-IRP2 Tg × Parkin KO mice (Fig. 3C). Electron microscopic analyses revealed the presence of neurons with condensed nuclei and round swollen mitochondria in the SN of 6-month-old NSE-IRP2 Tg × Parkin KO mice (Fig. 3D). These results indicate that the subtle increase of

IRP2 perturbs the integrity of the neurons by increasing mitochondrial oxidative insults and that Parkin is involved in the clearance of iron-induced oxidized mitochondrial proteins.

3.4 Decrease in dopaminergic neurons in the SN and locomotor dysfunctions in NSE-IRP2 Tg × Parkin KO mice

Selective loss of dopaminergic neurons in the SN is involved in the pathogenesis of Parkinson's disease and Parkin is a familial Parkinson's disease-related protein [3]. Consistent with neuronal degeneration in the SN (Fig. 3), the number of TH-positive cells was significantly lower in the SN of 5-month-old NSE-IRP2 Tg × Parkin KO mice (Fig. 4A and B). The amounts of dopamine and its metabolites were significantly lower in the striatum of 5-month-old NSE-IRP2 Tg × Parkin KO mice (Fig. 4C–E). Motor conditions are major symptoms of Parkinson's disease [3]. Consistent with loss of dopaminergic neurons in the SN, both horizontal activity and rearing scores in open-field tests were significantly lower in 5-month-old NSE-IRP2 Tg × Parkin KO mice (Fig. 4F and G). Collectively, these results clearly indicate that the subtle increase in exogenously expressed IRP2 and loss of Parkin synergistically accelerates the loss of dopaminergic neurons in the SN and provokes motor symptoms.

4. Discussion

Since induced expression of IRP2 increases the amount of iron that cannot be stored safely, we dissected the role of iron in neuronal damages using neuron-specific IRP2 Tg mice. Only subtle increase of IRP2 was enough for mitochondrial 4-HNE modification in mouse neurons (Fig. 1H) although IRP2 expression alone could not provoke mitochondrial 4-HNE modifications in transformed cells (Fig. 2A and F). Expression of IRP2 is subtle in neurons in NSE-IRP2 Tg mice, but it is continuous throughout their lifetime. Moreover, 4-HNE signals could be detected in 18-month-old, but not in 6-month-old in NSE-IRP2 Tg mice (Fig. 1H and 3A), which suggests that duration of IRP2 expression in quiescent neuronal cells may be a critical factor for iron-induced mitochondrial 4-HNE modifications. Since cultured cells proliferated rapidly, we evaluated the effect of iron on 4-HNE modifications within two days. Thus, we suspect that despite very trace, transgenic expression of IRP2 can induce the subtle, but chronic increase of iron that cannot be stored safely and result in mitochondrial oxidative insults and the deterioration of neurodegeneration in quiescent neurons.

Loss of Parkin enhanced accumulation of mitochondrial 4-HNE-modified proteins and degeneration of neurons of the SN in NSE-IRP2 Tg mice. Impaired clearance of oxidized mitochondrial proteins in the SN neurons appeared involved in Parkinson's disease-like phenotypes in NSE-IRP2 Tg × Parkin KO mice (Fig. 4). Additionally, Parkin is involved in the clearance of oxidatively modified proteins in mitochondria (Fig. 2F). However, mechanism underlying Parkin-mediated removal of mitochondrial 4-HNE modification is currently unknown because in iron-treated IRP2-expressing cultured cells, we could not detect mitophagy in that Parkin is shown to be involved [8, 11] (unpublished observation). Thus, the mitochondrial quality control, in which Parkin is involved, but possibly in a different mechanism from mitophagy, may play critical roles protecting dopaminergic neurons from iron-induced mitochondrial oxidative damages. Mitochondrial damages are suggested to function as triggering and accelerating factors in Parkinson's disease and accumulation of iron in the lesions of the disease is known [2]. Iron-induced mitochondrial oxidative damages might be involved in the development of Parkinson's disease.

Our results show that subtle increase of IRP2 is sufficient to induce mitochondrial oxidative insults. Thus, NSE-IRP2 Tg mice may be useful to probe the roles iron-induced mitochondrial oxidative insults in neurodegenerative disorders.

5. Conclusions

Expression of even trace amounts of IRP2 increased mitochondrial oxidative changes in neurons. The increase in IRP2 accelerates the loss of dopaminergic neurons in the SN and provokes motor symptoms of Parkin KO mice. NSE-IRP2 Tg mice may be suitable to probe the role of iron-induced mitochondrial oxidative damages in neurodegenerative disorders.

Acknowledgments

We thank Dr. Forss-Petter for pNSE. This work was partly supported by grants and a Grant-in-Aid for Scientific Research on Innovative Areas (Comprehensive Brain Science Network) from the Ministry of Education, Science, Sports and Culture of Japan to K.I. and M.K., respectively.

References

[1] M. Ashizuka, T. Fukuda, T. Nakamura, K. Shirasuna, K. Iwai, H. Izumi, K. Kohno, M. Kuwano, T. Uchiumi, Novel translational control through an iron-responsive element by interaction of multifunctional protein YB-1 and IRP2, Mol. Cell Biol. 22 (2002) 6375-6383.

[2] R.R. Crichton, D.T. Dexter, R.J. Ward, Brain iron metabolism and its perturbation in neurological diseases, J. Neural. Transm. 118 (2011) 301-314.

[3] D.W. Dickson, H. Braak, J.E. Duda, C. Duyckaerts, T. Gasser, G.M. Halliday, J. Hardy, J.B. Leverenz, K. Del Tredici, Z.K. Wszolek, I. Litvan, Neuropathological assessment of Parkinson's disease: refining the diagnostic criteria, Lancet Neurol. 8 (2009) 1150-1157.

[4] S. Forss-Petter, P.E. Danielson, S. Catsicas, E. Battenberg, J. Price, M. Nerenberg, J.G. Sutcliffe, Transgenic mice expressing β-galactosidase in mature neurons under neuron-specific enolase promoter control, Neuron 5 (1990) 187-197.

[5] K. Herrup, Y. Yang, Cell cycle regulation in the postmitotic neuron: oxymoron or new biology?, Nat. Rev. Neurosci. 8 (2007) 368-378.

[6] K. Iwai, R.D. Klausner, T.A. Rouault, Requirements for iron-regulated degradation of the RNA binding protein, iron regulatory protein 2, EMBO J. 14 (1995) 5350-5357.

[7] M. Koike, M. Shibata, M. Tadakoshi, K. Gotoh, M. Komatsu, S. Waguri, N. Kawahara, K. Kuida, S. Nagata, E. Kominami, K. Tanaka, Y. Uchiyama, Inhibition of autophagy prevents hippocampal pyramidal neuron death after hypoxic-ischemic injury, Am. J. Pathol. 172 (2008) 454-469.

[8] N. Matsuda, S. Sato, K. Shiba, K. Okatsu, K. Saisho, C.A. Gautier, Y.S. Sou, S. Saiki, S. Kawajiri, F. Sato, M. Kimura, M. Komatsu, N. Hattori, K. Tanaka, PINK1 stabilized by mitochondrial depolarization recruits Parkin to damaged mitochondria and activates latent Parkin for mitophagy, J. Cell Biol. 189 (2010) 211-221.

[9] E.G. Meyron-Holtz, M.C. Ghosh, K. Iwai, T. LaVaute, X. Brazzolotto, U.V. Berger, W. Land, H. Ollivierre-Wilson, A. Grinberg, P. Love, T.A. Rouault, Genetic ablations of iron regulatory proteins 1 and 2 reveal why iron regulatory protein 2 dominates iron homeostasis, EMBO J. 23 (2004) 386-395.

[10] T. Moroishi, M. Nishiyama, Y. Takeda, K. Iwai, K.I. Nakayama, The FBXL5-IRP2 axis is integral to control of iron metabolism in vivo, Cell Metab. 14 (2011) 339-351.

[11] D. Narendra, A. Tanaka, D.F. Suen, R.J. Youle, Parkin is recruited selectively to impaired mitochondria and promotes their autophagy, J. Cell Biol. 183 (2008) 795-803.

[12] W.D. Rausch, Y. Hirata, T. Nagatsu, P. Riederer, K. Jellinger, Tyrosine hydroxylase activity in caudate nucleus from Parkinson's disease: effects of iron and phosphorylating agents, J. Neurochem. 50 (1988) 202-208.

[13] J.R. Roede, D.P. Jones, Reactive Species and Mitochondrial Dysfunction: Mechanistic Significance of 4-Hydroxynonenal, Environ. Mol. Mutagen. 51 (2010) 380-390.

[14] T.A. Rouault, The role of iron regulatory proteins in mammalian iron homeostasis and disease, Nat.Chem. Biol. 2 (2006) 406-414.

[15] S. Sato, T. Chiba, S. Nishiyama, T. Kakiuchi, H. Tsukada, T. Hatano, T. Fukuda, Y. Yasoshima, N. Kai, K. Kobayashi, Y. Mizuno, K. Tanaka, N. Hattori, Decline of striatal dopamine release in parkin-deficient mice shown by ex vivo autoradiography, J. Neurosci. Res. 84 (2006) 1350-1357.

[16] E.A. Schon, S. Przedborski, Mitochondria: the next (neurode)generation, Neuron 70 (2011) 1033-1053.

[17] M.A. Smith, P.L. Harris, L.M. Sayre, G. Perry, Iron accumulation in Alzheimer disease is a source of redox-generated free radicals, Proc. Natl. Acad. Sci. USA 94 (1997) 9866-9868.
[18] M. Takanashi, H. Mochizuki, K. Yokomizo, N. Hattori, H. Mori, Y. Yamamura, Y. Mizuno, Iron accumulation in the substantia nigra of autosomal recessive juvenile parkinsonism (ARJP), Parkinsonism Relat. Disord. 7 (2001) 311-314.
[19] F. Tokunaga, S. Sakata, Y. Saeki, Y. Satomi, T. Kirisako, K. Kamei, T. Nakagawa, M. Kato, S. Murata, S. Yamaoka, M. Yamamoto, S. Akira, T. Takao, K. Tanaka, K. Iwai, Involvement of linear polyubiquitylation of NEMO in NF-κB activation, Nat. Cell Biol. 11 (2009) 123-132.
[20] N. Zarkovic, A. Cipak, M. Jaganjac, S. Borovic, K. Zarkovic, Pathophysiological relevance of aldehydic protein modifications, J. Proteomics 92 (2013) 239-247.
[21] L. Zecca, M.B. Youdim, P. Riederer, J.R. Connor, R.R. Crichton, Iron, brain ageing and neurodegenerative disorders, Nat. Rev. Neurosci. 5 (2004) 863-873.

Figure legends

Fig. 1. Generation of NSE-IRP2 Tg mice. (A) Schematic of the NSE-IRP2 transgene. (B) Genomic DNA was analyzed by Southern blotting. (C) Brain lysates from mice that were administered DFO were used for immunoprecipitation with anti-myc and probed with anti-IRP2. (D) Sections from 12-month-old mice were immunostained with anti-myc. Bar, 50 μm. (E) Lysates, as in (C) and lysates of RD4 cells expressing IRP2-myc were incubated with ^{32}P-labeled IRE and anti-myc, and the mixture was then separated by PAGE and analyzed by autoradiography. (F) Sections from12-month-old mice were stained using Turnbull's blue and DAB to detect ferrous iron. Bar, 50 μm. (G) Lysates from the striatum of 12-week-old mice were probed with anti-TH. (H) Sections from 18-month-old mice were immunostained with anti-4-HNE. Arrows indicates 4-HNE-modificated proteins. Bar, 200 μm.

Fig. 2. Induced expression of IRP2 augments iron-mediated mitochondrial damage. (A-D) HEK293 cells in which IRP2 expression was induced, or un-induced cells, were treated with the 100 μg/ml FAC for 12 h. Cells were analyzed by immunostaining as indicated (A), and line scan plot in FAC-treated cells expressing IRP2 and the percentage of 4-HNE-positive mitochondria were shown in (B) and (C), respectively (n=10). Cells were analyzed by MitoTracker staining (D). (E) Parkin-overexpressing HEK293 cells in which IRP2 expression was induced or un-induced, were incubated in the presence or absence of 100 μg/ml FAC for 9 h. Lysates were probed by immunoblotting. (F and G) HeLa cells expressing IRP2 and/or Parkin were treated with 50 μg/ml FAC. Cells were analyzed by immunofluorescence staining (F) and the percentage of 4-HNE-positive mitochondria was shown (G) (n=10). Bars, 10 μm. **, $P < 0.01$.

Fig. 3. IRP2 increased mitochondrial oxidative insults and neurodegeneration in the SN. (A and B) Sections of the SN from 6-month-old mice were immunostained with as indicated antibodies. The percentage of 4-HNE-positive mitochondria was shown (B) (n=10). Bar, 50 μm. **, $P < 0.01$. (C) Semi-thin sections of the SN from 6-month-old mice of were stained with toluidine blue. In the double-mutant mice, dying neurons that show shrinkage are intensely stained with toluidine blue (arrows). Bar, 20 μm. (D) Electron micrographic analysis of neurons in the SN from 6-month-old mice. In the double-mutant mouse, a dying neuron with increased electron

density is shrunken and contains round swollen mitochondria with an electron-lucent matrix and a nucleus with a large peculiarly shaped nucleolus. Bar, 5 μm (left) and 1 μm (right).

Fig. 4. IRP2 accelerates the progression of Parkin-induced symptoms. (A and B) Sections of the SN from 5-month-old mice were immunostained with anti-TH (A) and the number of TH-positive cells was quantified (B) (n=10). Bar, 1 mm. (C–E) Concentrations of dopamine (C) DOPAC (D), and HVA (E) in the striata of 5-month-old mice were measured (n=15). (F and G) The horizontal activity (F) and rearing activity (G) of 5-month-old mice were measured using the open-field test scored over a 5 min period (n=15). *, $P < 0.05$.

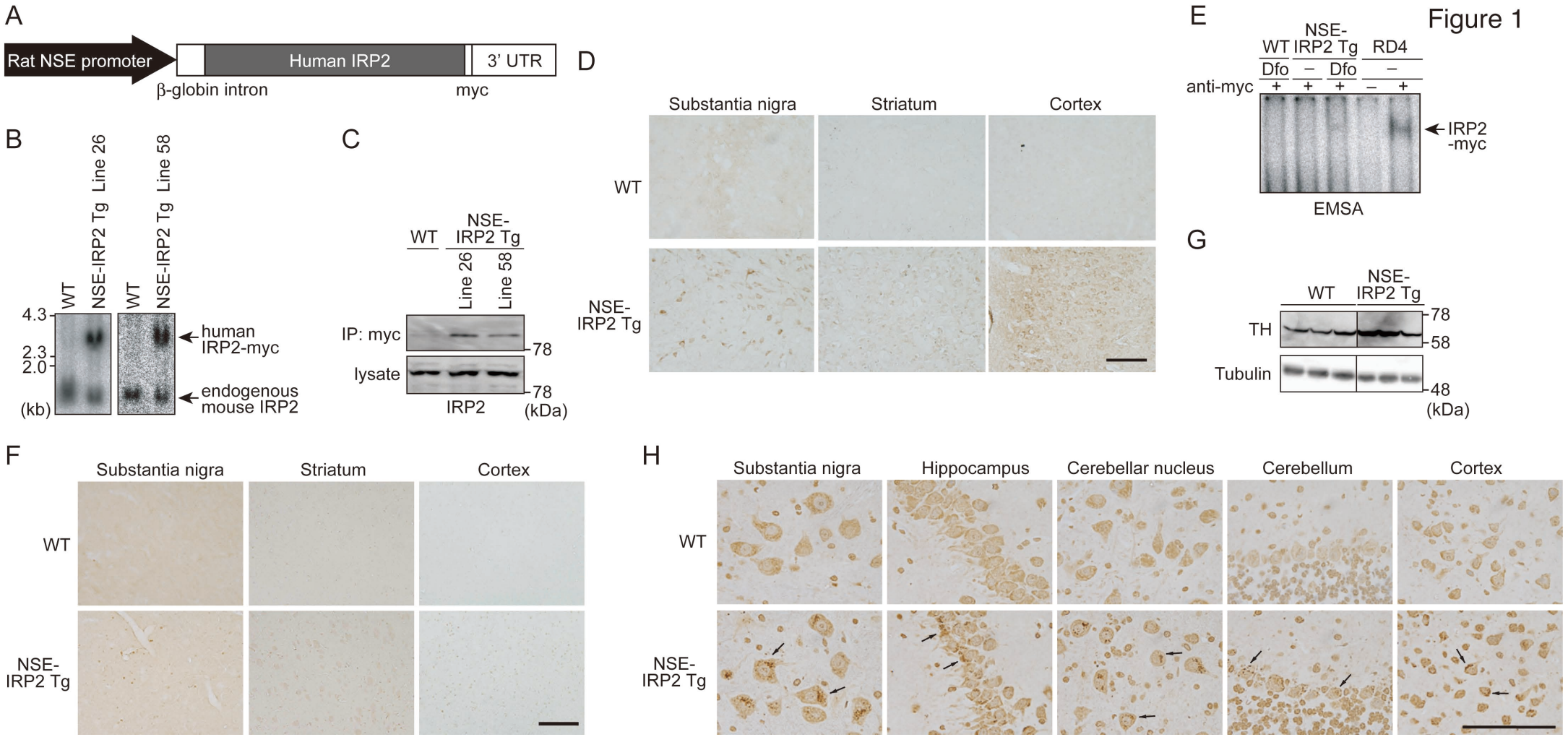
A
Rat NSE promoter
Human IRP2
3' UTR
β-globin intron
myc
B
WT
NSE-IRP2 Tg Line 26
WT
NSE-IRP2 Tg Line 58
4.3
2.3
2.0
(kb)
human IRP2-myc
endogenous mouse IRP2
C
WT
NSE-IRP2 Tg
Line 26
Line 58
IP: myc
lysate
78
78
IRP2
(kDa)
D
Substantia nigra
Striatum
Cortex
WT
NSE-IRP2 Tg
E
WT
NSE-IRP2 Tg
RD4
Dfo
–
Dfo
–
anti-myc
+
+
+
–
+
IRP2 -myc
EMSA
G
WT
NSE-IRP2 Tg
TH
Tubulin
78
58
48
(kDa)
F
Substantia nigra
Striatum
Cortex
WT
NSE-IRP2 Tg
H
Substantia nigra
Hippocampus
Cerebellar nucleus
Cerebellum
Cortex
WT
NSE-IRP2 Tg

Figure 1

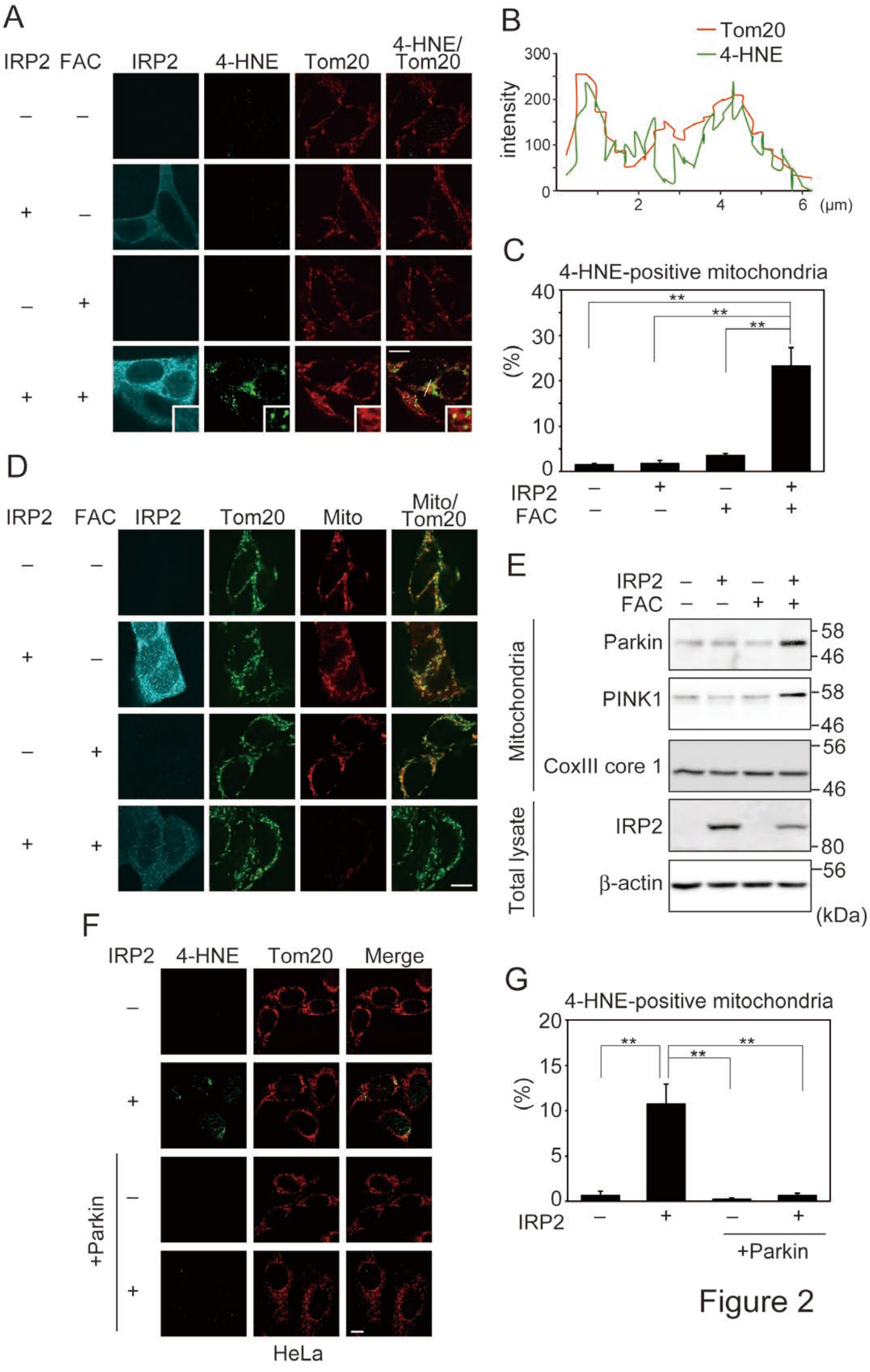
A
IRP2 FAC
IRP2
4-HNE
Tom20
4-HNE/ Tom20
B
Tom20
4-HNE
intensity
300
200
100
0
2
4
6 (μm)
C
4-HNE-positive mitochondria
40
30
20
10
0
(%)
**
**
**
IRP2 – + – +
FAC – – + +
D
IRP2 FAC
IRP2
Tom20
Mito
Mito/ Tom20
E
IRP2 – + – +
FAC – – + +
Mitochondria
Parkin
PINK1
CoxIII core 1
Total lysate
IRP2
β-actin
58
46
58
46
56
46
80
56
(kDa)
F
IRP2
4-HNE
Tom20
Merge
+Parkin
HeLa
G
4-HNE-positive mitochondria
20
15
10
5
0
(%)
**
**
**
IRP2 – + – +
+Parkin

Figure 2

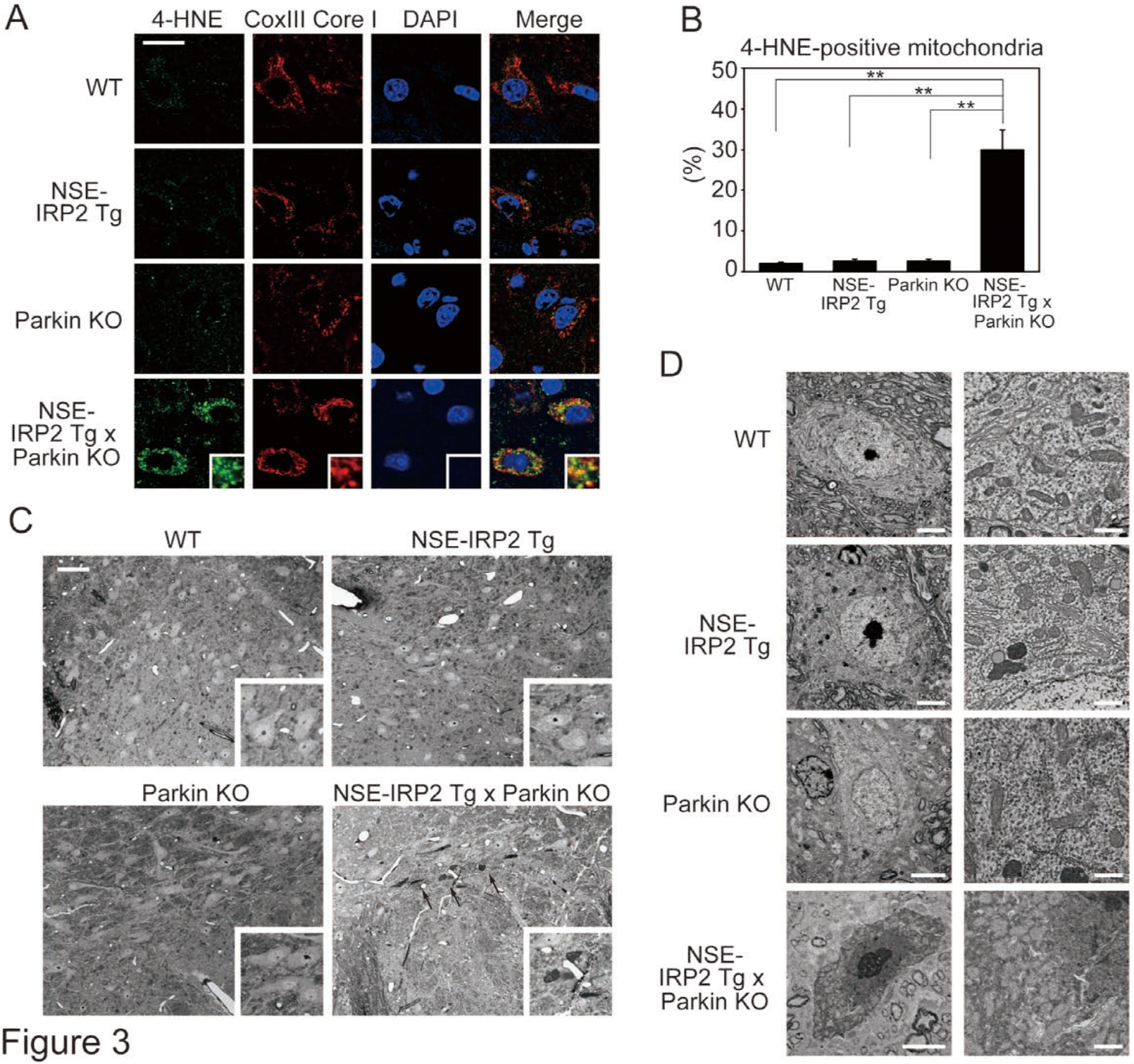
A
4-HNE
CoxIII Core I
DAPI
Merge
WT
NSE-IRP2 Tg
Parkin KO
NSE-IRP2 Tg x Parkin KO
B
4-HNE-positive mitochondria
(%)
50
40
30
20
10
0
**
**
**
WT
NSE-IRP2 Tg
Parkin KO
NSE-IRP2 Tg x Parkin KO
C
WT
NSE-IRP2 Tg
Parkin KO
NSE-IRP2 Tg x Parkin KO
D
WT
NSE-IRP2 Tg
Parkin KO
NSE-IRP2 Tg x Parkin KO

Figure 3

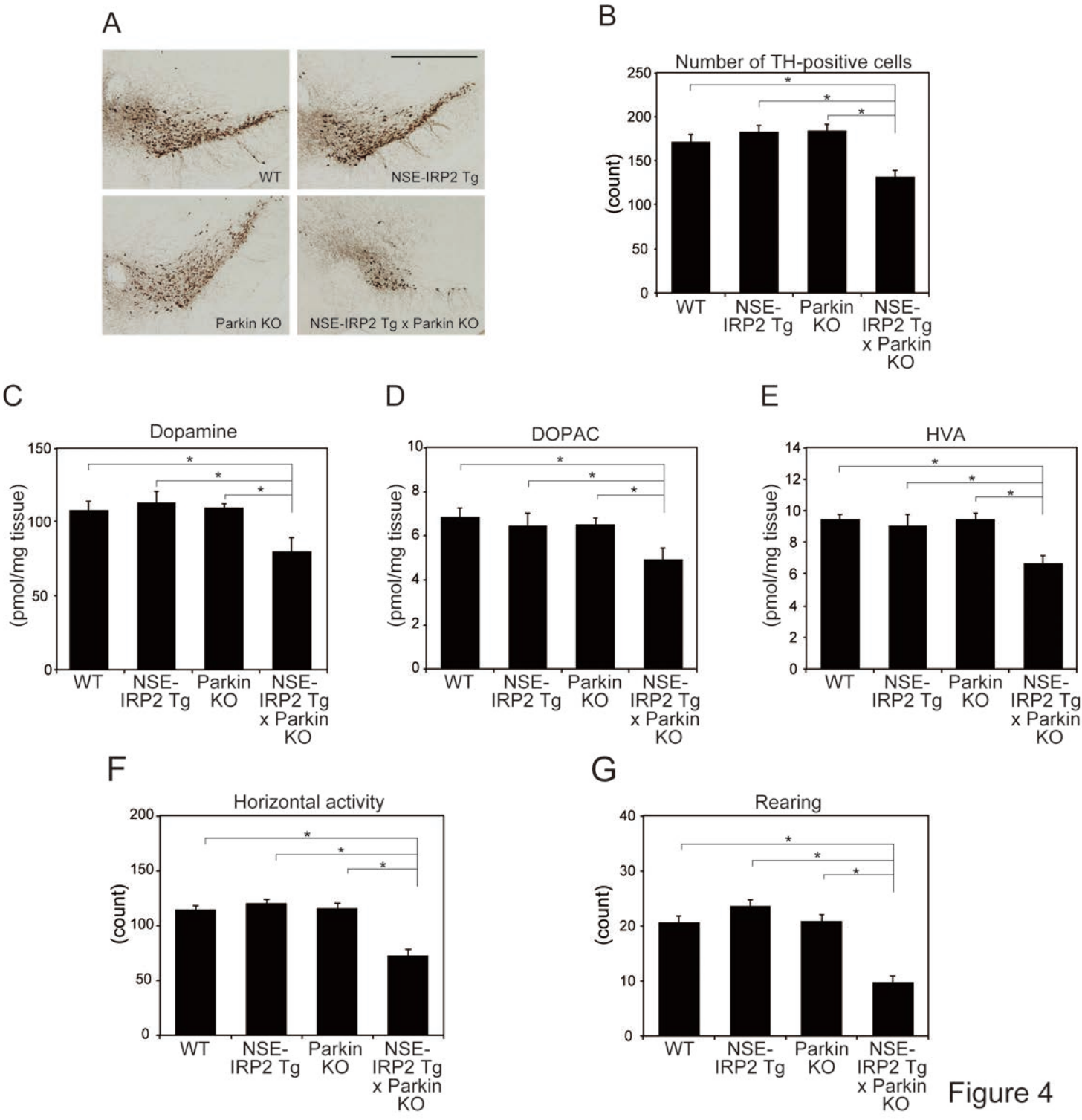
A
WT
NSE-IRP2 Tg
Parkin KO
NSE-IRP2 Tg x Parkin KO
B
Number of TH-positive cells
(count)
250
200
150
100
50
0
WT
NSE-IRP2 Tg
Parkin KO
NSE-IRP2 Tg x Parkin KO
C
Dopamine
(pmol/mg tissue)
150
100
50
0
D
DOPAC
10
8
6
4
2
E
HVA
14
12
F
Horizontal activity
G
Rearing
40
30
20
10

Figure 4